ELSEVIER

Journal of Nuclear Materials 241–243 (1997) 914–918

journal of nuclear materials

SOL parameters and local transport in the FTU tokamak

M. Leigheb [a,*], V. Pericoli Ridolfini [a], R. Zagórski [a,b]

[a] *ENEA, Centro Ricerche, C.P. 65, 00044 Frascati (Rome), Italy*
[b] *Institute of Plasma Physics and Laser Microfusion, Warsaw, Poland*

Abstract

Poloidal asymmetries in the FTU scrape off layer (SOL) can be as high as factor 2 for density, electron temperature and their e-folding decay lengths. The insertion of an additional limiter demonstrates a strong correlation with the corresponding variation of the magnetic connection length. This and the data analysis with the 2D multifluid SOL code EPIT indicate that transport is affected by the change of the local SOL temperature. The SOL plasma appears to be not affected changing the first wall material from inconel to silicon.

Keywords: FTU; SOL plasma; Tokamak; Langmuir probe

1. Introduction

Understanding the behavior of the tokamak scrape off layer (SOL) plasma is crucial for the divertor physics in a fusion reactor. However information on the SOL quantities, on their link with the bulk plasma and on the local transport properties are still not very abundant. Here we study the dependence on the poloidal angle θ of the FTU SOL quantities and their variation with the bulk plasma, comparing the experimental results with the predictions of a 2D multifluid code. The interest of the work lies on the FTU SOL characteristics some of which are reactor relevant already in Ohmic regime: densities at the last closed magnetic surface (LCMS) $n_{eL} \approx 1 \cdot 10^{20}$ m^{-3}, power fluxes into the SOL ≈ 0.1 MW/m^2, and onto the limiter surface ≈ 5 MW/m^2 are often observed.

In Section 2 the poloidal asymmetries are described and interpreted; in Section 3 the link of the SOL with the bulk plasma and the effect of the limiter material are discussed; in Section 4 conclusions are given.

2. Poloidal asymmetries

Strong poloidal asymmetries were first observed on Alcator C [1]. Their cause in FTU was previously proposed to be the poloidal variation of the magnetic connection length L_c [2]. This variation is inevitable in a poloidal limiter tokamak when the LCMS shape does not match exactly the limiter, and it is further exalted if the limiter is not poloidally continuous as in FTU. Indeed a field line close to LCMS may run several toroidal turns before hitting the limiter. To support with more accuracy this hypothesis the variation of L_c was controlled independently of the plasma parameters with an additional limiter and the SOL was sampled on a finer spatial scale with a reciprocating Langmuir probe built on purpose. The head probe carries 33 electrodes and extends over $\Delta\theta \approx 75°$ across the outer equatorial plane. The study was carried out comparing radial and poloidal profiles of the SOL quantities for shots identical except for the presence of the second limiter, and then analyzing the causes of the differences. With this method the SOL plasma is changed without affecting the bulk, then the study of the energy and particles transport as a function of the local SOL parameters becomes easier.

The experimental results are summarized in Fig. 1a–f where the following quantities are plotted versus θ. (a): $2 \cdot L_c$, i.e. the total magnetic line length; (b), (c): n_{eL} and T_{eL}, density and temperature at LCMS; (d) $\tilde{n}_{eL} = \langle \delta n_{eL}^2 \rangle^{1/2} / n_{eL}$: the relative density fluctuation level at LCMS; (e), (f): λ_n, λ_T: n_e and T_e e-folding decay lengths. The connection lengths are evaluated tracking the magnetic field lines connected to each probe until a material obstacle is struck, then averaging over a radial depth of 1.5

* Corresponding author. Tel.: +39-6 9400 5431; fax: +39-6 9400 5735; e-mail: leigheb@frascati.enea.it.

PII S0022-3115(96)00631-9

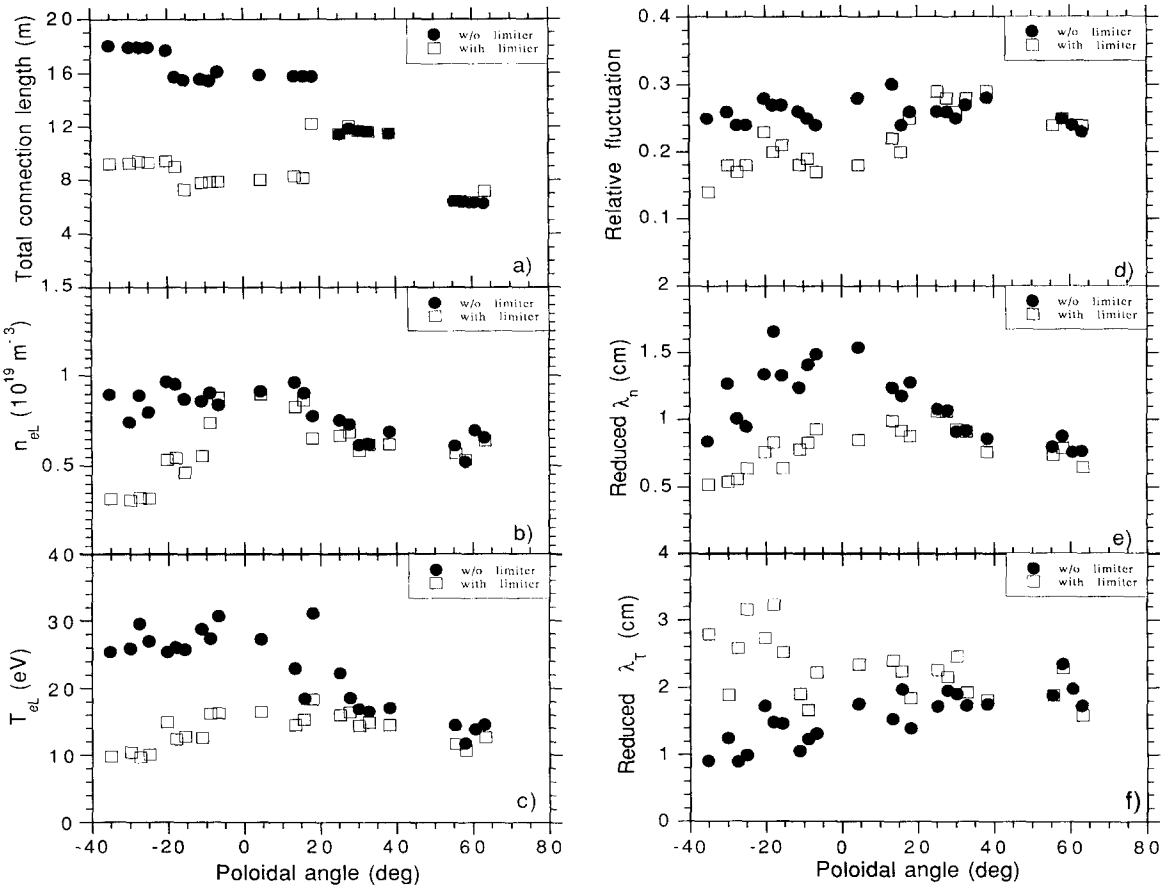

Fig. 1. Plot versus the poloidal angle θ of: (a) $2 \cdot L_c$, total connection length, (b) density at the LCMS; (c) electron temperature at LCMS; (d) relative fluctuation level averaged within the SOL; (e) $\lambda_n \cdot (\pi R_0/L_c)^{1/2}$, reduced density e-folding decay length; (f) $\lambda_T \cdot (\pi R_0/L_c)^{1/2}$, reduced temperature e-folding decay length. Open symbols: additional limiter inserted, full symbols: additional limiter extracted. Shot parameters: $\bar{n}_e \approx 0.8 \cdot 10^{20}$ m^{-3}, $I_p = 0.7$ MA, $B_T = 5.8$ T.

cm outside LCMS. The λ are corrected for the flux expansion along θ and divided by the ratio $(L_c/\pi R_0)^{1/2}$, where R_0 is the tokamak major radius, in order to be free from first order geometrical effects, see Ref. [3]. These reduced λ are linked directly to the transport in the SOL and should remain constant unless the transport coefficients vary. Two consecutive shots with the additional limiter extracted (full symbols) or inserted (open symbols) are compared; for both, line averaged density is $\bar{n}_e \approx 0.8 \cdot 10^{20}$ m^{-3}, plasma current $I_p = 0.7$ MA and toroidal magnetic field $B_T = -5.8$ T.

The insertion of the second limiter causes for $\theta < 18°$ a sudden reduction of L_c, which otherwise would be a quite regular function of the poloidal angle, Fig. 1a, and causes significant differences only in this SOL region under its shadow: all the quantities react immediately to the presence of this limiter except n_{eL}. The reason of this θ shift is not understood at present, probably convective flows arise in the SOL to smooth out the discontinuity due to the additional limiter, but originating form the quite cold nearby plasma, Fig. 1c, compensate only the decrease of the density.

When the limiter is extracted both n_{eL} and T_{eL} rise then saturate moving from short to long L_c, λ_n shows a clear increase around the equator ($\theta \approx 0°$) and λ_T regularly decreases. This behavior of λ_n in a region where n_{eL} and T_{eL} are quite constant ($\theta < 18°$) and the fact that the ratio $\lambda_n(0°)/\lambda_n(-40°)$ is close to 1.8 for both shots suggest that the poloidal position itself influences the particle transport. Simple reasons for that are not supported by the data: no similar θ profiles of the electrostatic turbulence from $\tilde{n}_{eL}$ measurements, too small variation of the magnetic field (< 10%) for a Bohm type diffusion. Possible effect due to the magnetic topology are under investigation.

The behavior of λ_n and λ_T with L_c and their different reaction to the presence of the second limiter indicate that the SOL conditions act oppositely on the particles and heat transport. The θ shift of the response of n_{eL} to the limiter insertion suggests that the main parameter is the electron temperature: particle transport increases with T_e, as sup-

ported also by the higher fluctuation level for the shot without limiter, while heat transport decreases. The ratio $\chi_{e\perp}/D_\perp$ of the electron thermal conductivity to the perpendicular particle diffusion coefficient, should vary from 10 to 1 for the data of Fig. 1, according to the usual relation [3] with λ_T/λ_n, which in turn varies from about 4 to 1.

Simple balance equations in the SOL predict only $n_{eL} \propto L_c^{0.5}$, close to experiment, while for T_{eL} no variation with L_c is foreseen. Indeed, if tile radiation losses and e–i coupling are negligible, as indicated by the 2D multifluid EPIT code [4] for the case of Fig. 1, $c_s = [(T_e + T_i)/m_i]^{0.5}$ is the ion sound velocity, and λ' are the usual non reduced e-folding lengths, for energy $1/\lambda'_E = 1/\lambda'_n + 1.5/\lambda'_T$, the particles and electron energy balance equations when also ionization is negligible, read respectively as:

$$0.5 \cdot c_s \cdot n_{eL} \cdot \lambda'_n = \Phi_\perp \cdot L_c \quad (1a)$$

$$\gamma_e \cdot c_s \cdot n_{eL} \cdot T_{eL} \cdot \lambda'_E = 0.5 \cdot Q_\perp \cdot L_c \quad (1b)$$

where γ_e is the electron sheath transmission factor, $\Phi_\perp$ is the particle outflux density and $Q_\perp$ is the SOL input power flux density, half of which is carried by electrons. The factor 0.5 in Eq. (1a) accounts for the density reduction along the flux tube. Assuming [3] $\lambda'_n = (D_\perp \cdot L_c/c_s)^{0.5}$ one has:

$$n_{eL} = 2 \cdot \Phi_\perp \cdot [L_c/(c_s \cdot D_\perp)]^{0.5} \quad (2)$$

$$T_{eL} = 0.25/\gamma_e \cdot Q_\perp/\Phi_\perp \cdot (1 + 1.5 \cdot \lambda'_n/\lambda'_T) \quad (3)$$

Approximately n_{eL} is proportional to $L_c^{0.5}$, because c_s is a weak function of T_e since $T_i > T_e$ due to the low e–i coupling, while T_{eL} is nearly constant because the ratio λ'_n/λ'_T is independent of L_c.

To gain more quantitative information and discriminate 2D effects from those due to the variation of the transport coefficient, the SOL behavior has been simulated with EPIT code. The results are presented in Fig. 2a–c where the following quantities are plotted versus L_c: n_{eL} (a), T_{eL} (b), λ_n and λ_T (c). The code inputs are: $P_{SOL} = 0.3$ MW, $\chi_{e\perp} = 2$ m^2/s, $\chi_{i\perp}^{0.4}$ m^2/s, $D_\perp = 1$ m^2/s, total particle flux into the SOL $\Gamma_\perp = 4, 5, 6 \cdot 10^{21}$ s^{-1}, nickel as the main impurity ($Z_i = 28$). All quantities, LCMS density, temperature and reduced e-folding lengths, vary with L_c, as experimentally observed moving along θ, see Fig. 1. Quantitatively the agreement is within a factor 1.2 for n_{eL}, while T_{eL} rises substantially less than the experimental factor 2.5 ÷ 3, and both the reduced λ vary slower than observed. Therefore, considering that terms as ionization,

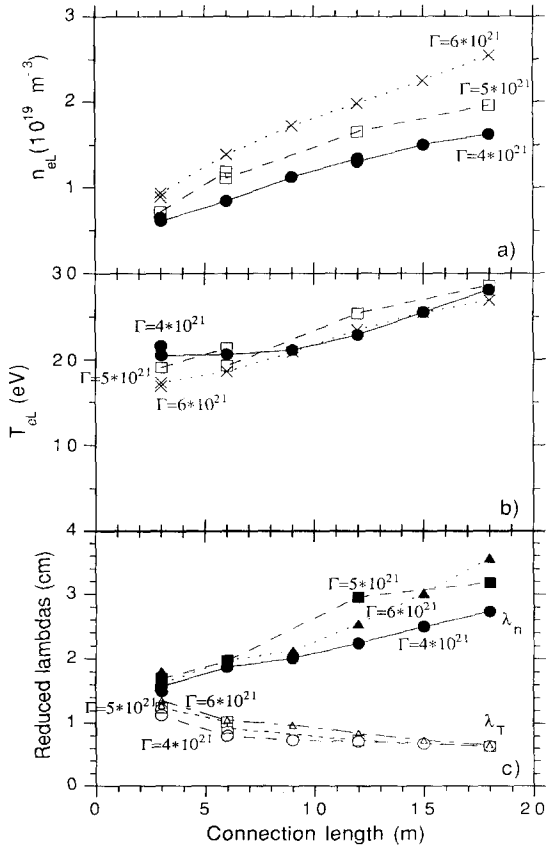

Fig. 2. Plot versus L_c of the 2D EPIT code results: (a) density at the LCMS; (b) electron temperature at LCMS; (c) λ_n and λ_T, density and temperature e-folding decay lengths normalized to $(L_c/\pi R_0)^{1/2}$. EPIT input parameters: three particle outflow: $\Gamma_\perp = 4, 5, 6 \cdot 10^{21}$ s^{-1}, specified in the figure, $P_{SOL} = 0.3$ MW, $\chi_{e\perp} = ^2$ m^2/s, $\chi_{i\perp} = 0.4$ m^2/s, $D_\perp = 1$ m^2/s.

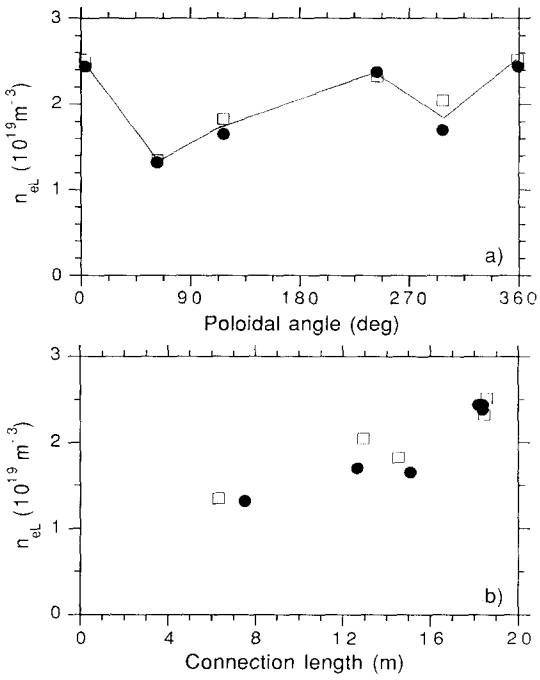

Fig. 3. Plot of the density at LCMS: (a) along the poloidal circumference, (b) as a function of the connection length, for two very similar shots: $\bar{n}_e \approx 0.94 \cdot 10^{20}$ m^{-3}, $I_p = 0.6$ MA, $B_T = 5.7$ T, $P_{SOL} \approx 0.34$ MW.

radiation cooling and e–i coupling result small from the simulations as said above, 2D effects actually modify T_{eL}, λ_n and λ_T, but negligibly n_{eL}, in the same direction as experimentally observed, but are not enough to match quantitatively the experiment. At $L_c = 10$ m the λ are rather near to the experimental values, while λ_n should be depressed and λ_T raised by a factor ≈ 2 at $L_c = 3$ m. According to several others EPIT simulations this implies 4 times reduction of $D_\perp$ and about 10 times increase of $\chi_{e\perp}$, i.e. $D_\perp \approx 0.25$ m^2/s and $\chi_{e\perp} \approx {}^{20}$ m^2/s. This last factor, even if affected by other code input parameters, mainly $\Gamma_\perp$, would also produce the correct magnitude of T_{eL} at $L_c = 3$ m.

The primary effect of the poloidal variation of the connection length on SOL asymmetries is confirmed for almost the whole plasma circumference by the measurements shown in Fig. 3a, b. The LCMS density sampled at $\theta = 0°$, 60°, 110°, 220°, 295° is plotted versus either θ or L_c for two similar shots with $\bar{n}_e \approx 0.94 \cdot 10^{20}$ m^{-3}, $I_p = 0.6$ MA, $B_T = 5.7$ T, $P_{SOL} \approx 0.34$ MW: the high degree of correlation in Fig. 3b is evident.

3. Link with bulk plasma

A parametric search with EPIT has been carried out in the space of the code input quantities within the boundaries $\Gamma_\perp = 1–70 \cdot 10^{21}$ s^{-1}, $L_c = 3–18$ m, $P_{SOL} = 0.15–1$ MW, $D_\perp = 0.25–1$ m^2/s, $\chi_{e\perp} = 2–15$ m^2/s, in order to isolate the most important of them for the SOL density and temperature. According the linear regression analysis the following relations hold:

$$n_{eL} \propto \Gamma_\perp^{0.9} \cdot L_c^{0.5} \cdot D_\perp^{-0.45} \tag{4}$$

$$T_{eL} \propto P_{SOL}^{0.4} \cdot \Gamma_\perp^{-0.4} \cdot L_c^{0.2} \cdot D_\perp^{0.12} \tag{5}$$

If we compare Eqs. (4) and (5) with Eqs. (2) and (3) respectively, we see that 2D effects and the consideration of the exact equations governing the SOL are important for temperature at LCMS, but not for density. This fact noted above is now valid for the whole parameter space considered. The milder power dependence of T_{eL} on the ratio $P_{SOL}/\Gamma_\perp$ ($\propto Q_\perp/\Phi_\perp$) is due to a self regulating mechanism [4]: when P_{SOL} rises the amount of sputtered impurities increases and with it radiation cooling, which depresses T_e; when instead $\Gamma_\perp$ rises the higher e–i coupling tends to heat electrons. The L_c and $D_\perp$ terms are in general due to both 2D effects and impurity dynamics: the increase of impurity screening with L_c, observed in FTU [6], may imply less radiation cooling and hence higher T_e. Experimentally, for bulk plasma quantities ranging in $\bar{n}_e$: $0.2 \div 2 \cdot 10^{20}$ m^3, I_p: $0.3 \div 1.0$ MA, B_T: $3.8 \div 7.1$ T, the following laws hold (Fig. 4a, b):

$$n_{eL} = 2.46 \cdot 10^{-9} \cdot \left(\bar{n}_e/f_{pk}\right)^{1.36} \cdot L_c^{0.96} \tag{6}$$

$$T_{eL} = 2.09 \cdot \lambda_T^{-0.41} \cdot L_c^{0.27}/f_{pk}^{0.21} \tag{7}$$

The units are MKS and f_{pk} is the density peaking factor $n_{e0}/\bar{n}_e$. All the quantities found in Eq. (6) can be recognized also in Eq. (4): indeed $D_\perp$ is tightly linked to L_c, see Section 2, and f_{pk}, and $\Gamma_\perp$ to $\bar{n}_e$ and f_{pk}. The power dependence on $\bar{n}_e$ in Eq. (6) confirms previous results [2] when L_c was not included in the analysis. From Ref. [5] one has approximated that $\Gamma_\perp = D_\perp \cdot [n_e(\lambda_{iH}) - n_{eL}]/\lambda_{iH}$, where λ_{iH} is the neutral ionization mean free path and distances are counted from the LCMS radius inboard. Assuming $\lambda_{iH} \propto 1/n_e(\lambda_{iH})$, $\Gamma_\perp$ is $\propto D_\perp \cdot n_e^2(\lambda_{iH}) \propto D_\perp \cdot (\bar{n}_e/f_{pk})^2$, then inserting it into Eq. (4) it appears that the usual assumption $\Gamma_\perp \propto \bar{n}_e^2$ gives a too high dependence on $\bar{n}_e$ and that the almost linear dependence of n_{eL} on L_c can be explained if approximately $D_\perp \propto L_c$, in agreement with the results of Section 2 but over a variation of an order of magnitude of $\bar{n}_e$.

On the other hand, in the scaling of T_{eL} the exponent of L_c is near to that resulting from EPIT calculations. The lack of bulk plasma quantities mainly of $\bar{n}_e$ and P_{SOL} is not surprising if we consider that in the FTU data base the ratio of the energy to particle flux is almost constant and therefore when $\lambda_n \approx \lambda_T$ the only dependence left to temperature is to decrease as its e-folding length is increased, according to Eq. (3).

Substituting silicon to inconel as first wall material has allowed to increase the ratio $Q_\perp/\Phi_\perp$ [7], which according to Eq. (6) should raise T_{eL}, leaving unaltered n_{eL}. However within the experimental errors no difference is

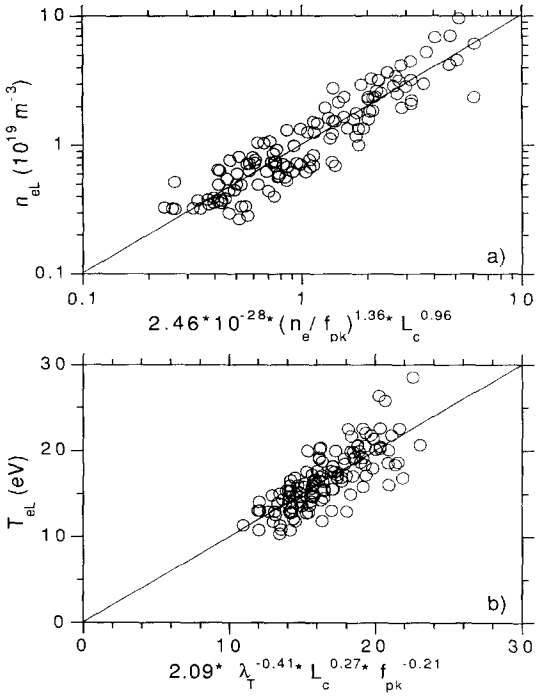

Fig. 4. Linear regression analysis on the experimental data for: (a) n_{eL}; (b) T_{eL}. The regression parameter is given in the label of the abscissa.

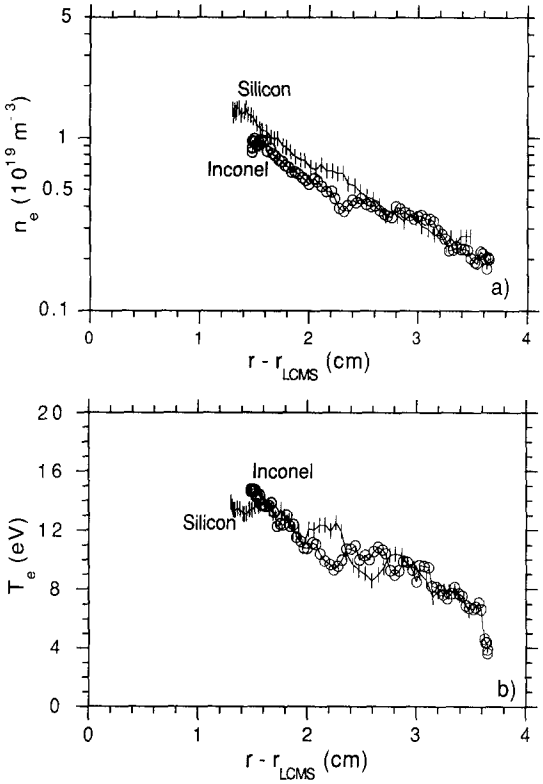

Fig. 5. Experimental SOL radial profiles of density (a), and electron temperature (b), plotted versus the distance from LCMS for two similar shots with $\bar{n}_e \approx 0.9 \cdot 10^{20}$ m^{-3}, $I_p = 0.7$ MA, $B_T = 5.8$ T, $L_c \approx 4.4$ m, but different first wall material, circles: Ni, $P_{SOL} \approx 0.3$ MW; crosses: Si, $P_{SOL} \approx 0.5$ MW).

found either for n_e or T_e in the SOL, as it happens for the bulk plasma quantities except the radiated power [7,8]. Fig. 5 compares n_e and T_e profiles in the SOL for two shots with $\bar{n}_e = 0.9 \cdot 10^{20}$ m^{-3}, $I_p = 0.7$ MA, $B_T = 5.8$ T, $L_c \approx 4.4$ m, same fuelling rate, i.e. same $\Phi_\perp$, but $P_{SOL} \approx 0.3$ MW, for the shot with inconel (circles) and ≈ 0.5 MW for that with silicon (bars). EPIT code predicts for the shot with Si an increase of the SOL electron temperature of about 8–9 eV which is not observed. The reason for this discrepancy is still an open question.

4. Conclusions

Poloidal asymmetries can be as high as a factor 2 for density, temperature and their reduced e-folding lengths in the FTU SOL plasma. Correlation with the poloidal variation of the magnetic connection length is evident, but the outer equatorial region still shows an enhanced transport. 2D effects and impurity dynamics correctly considered in the EPIT code can explain the type of variation but not its magnitude for T_{eL} and λ, unless the transport coefficients $D_\perp$ and $\chi_{e\perp}$, are allowed to vary. Experimentally these react in the opposite way to SOL changes and appear to depend more on temperature than on density. Simulations suggest that if T_{eL} goes from 10 to 30 eV, $D_\perp$ should increase from about 0.25 to 1 m^2/s and $\chi_{e\perp}$ should decrease from 20 to 2 m^2/s.

EPIT predictions agree satisfactorily with the experimental scaling law for the SOL density, while for the temperature the discrepancy is explained by the fact that in the experiment particle and energy fluxes are not independent parameters. However even when the two fluxes are decoupled changing the first wall material from Ni to Si, no significant difference is observed in the SOL plasma, as it is for the bulk. This can be due to the coupling between SOL and main plasma not considered by the code, but it is still an unresolved problem.

References

[1] B. La Bombard and B. Lipschultz, Nucl. Fusion 27 (1987) 81.
[2] V. Pericoli Ridolfini, R. Zagórski et al., J. Nucl. Mater. 220–222 (1995) 218.
[3] P.C. Stangeby and G.M. McCracken, Nucl. Fusion 30 (1990) 1225.
[4] R. Zagórski, V. Pericoli Ridolfini and L. Pieroni, Control. Plasma Phys. 34 (1994) 466.
[5] P.C. Stangeby, J. Nucl. Mater. 145–147 (1987) 105.
[6] R. Bartiromo et al., Nucl. Fusion 35 (1995) 1161.
[7] M.L. Apicella et al., Nucl. Fusion, to be published; also as ENEA report: RT/ERG/FUS/95/19, Frascati (Roma) (1995).
[8] F. Alladio et al., Plasma Phys. Control. Fusion 36 (1994) B253.